Towards a Network-based Approach to Analyze Particle Swarm Optimizers

Marcos Oliveira
BioComplex Laboratory
Florida Institute of Technology
Melbourne, USA
moliveirajun2013@my.fit.edu

Carmelo J. A. Bastos-Filho
Escola Politécnica de Pernambuco
University of Pernambuco
Recife, Brazil
carmelofilho@ieee.org

Ronaldo Menezes
BioComplex Laboratory
Florida Institute of Technology
Melbourne, USA
rmenezes@cs.fit.edu

***Abstract*—In Particle Swarm Optimizers (PSO), the way particles communicate plays an important role on their search behavior influencing the trade-off between exploration and exploitation. The interactions boundaries defined by the swarm topology is an example of this influence. For instance, a swarm with the ring topology tends to explore the environment more than with the fully connected global topology. On the other hand, more connected topologies tend to present a higher exploitation capability. We propose that the analysis of the particles interactions can be used to assess the swarm search mode, without the need for any particles properties (*e.g.* the particle's position, the particle's velocity, etc.). We define the weighted swarm influence graph $I_t^{t_w}$ that keeps track of the interactions from the last t_w iterations before a given iteration t. We show that the search mode of the swarm does have a signature on this graph based on the analysis of its components and the distribution of the node strengths.**

I. Introduction

Particle swarm optimization (PSO) is a computational intelligence technique inspired on the social behavior of flocks of birds and it is widely used to solve optimization problems with continuous variables [1]. The PSO algorithm consists of a population (swarm) of simple reactive agents (particles) that explore the search space by seeking the best solutions. Each particle has a position that represents a candidate solution for the problem and keeps the best position visited and the best position found by its neighbors, then they update their position based on this information. The swarm communication topology defines the particle neighborhood, which is the subset of particles each particle can exchange information with. The topology defines how the information is shared among the particles.

The way particles communicate plays an important role on the swarm behavior [2]. A proxy of this aspect may be seen, for instance, when the swarm topology is analyzed. The convergence speed and the quality of the solution obtained by the algorithm are influenced by the structure of the swarm topology [3], [4]. Less connected topologies slow down the information flow given that the information is transmitted indirectly through intermediary particles [4]. Conversely, highly connected topologies decrease the average distance between any pair of individuals. As a consequence, there is a tendency for the whole swarm to move quickly towards local optima. These two different behaviors are also related to the exploration-exploitation balance in the swarm. The exploration mode is the ability of individuals to broadly explore a region in the search space, while exploitation happens when the search is focused on a specific area of the search space [5]. The exploration-exploitation balance is not only related to the information exchange dynamics between particles, but can also be controlled by the equations used to update the particles features [3], [6].

However, although some researchers used the swarm topology to analyze the swarm behavior, this static structure provides only the limits of communication [2], [4]. Actually, the communication between particles changes at each iteration, since each particle selects the best neighbor to exchange information by using the current status in each iteration. Despite the lack of literature on this kind of analysis, Oliveira et al. proposed to understand the actual flow of information by defining the swarm influence graph, which is a graph with the nodes (particles) connected if they share information in a given iteration [7]. Nevertheless, this definition does not capture information flow dynamics from all iterations or a window containing consecutive iterations, but only the current one.

The usefulness of the influence graph relies on the capability to assess the influence of leading particles over the other particles along the iterations. The idea is that once particles move based on these interactions, the state of the swarm can be assessed by analyzing the network of these interactions, *i.e.* the influence graph. For example, one could assess the search mode of a swarm by using such analysis. The benefit of this approach is that properties of the particles (*e.g.* the particle's position, the particle's velocity, etc.) do not need to be taken into account in any cumbersome calculation for the assessment of the search behavior, just the interactions among the particles [8].

Therefore, we want to propose a network-based approach to assess the behavior of the swarm. This approach must allow one to include the history of particles interactions in order to capture the information flow dynamics of the swarm as a whole. Thus, we propose the weighted swarm influence graph $I_t^{t_w}$ that takes into account the last t_w iterations before a given iteration t. We simulate the PSO algorithm with four different topologies, known by their search modes, and we show that the swarm mode has a signature on the swarm influence graph based on the analysis of its components and its distribution of node strengths.

The paper is organized as follows: we briefly review the PSO and a simple swarm influence definition in Section II.

We propose, in Section III, the weighted swarm influence with a window of iterations. The simulation setup and results are presented in Section IV. Finally, we provide our conclusions and suggest some future works in Section V.

II. Background

In this section, a brief explanation of the topics related to this paper is given. In Section II-A, the standard Particle Swarm Optimization is described focusing on the topologies used by the swarm. The definition of the swarm influence graph is given in Section II-B.

A. Particle Swarm Optimization

Particle Swarm Optimization (PSO) is a stochastic, bio-inspired, population-based global optimization technique [1]. Each particle i contains four vectors in the D-dimensional space at iteration t: its current position in $\vec{x_i}$, its best position found so far $\vec{p_i}$, its velocity $\vec{v_i}$ and the best position found by its neighborhood $\vec{n_i}$. Each particle updates its position according to the current velocity $\vec{v_i}(t)$, the best position found by itself $\vec{p_i}(t)$ and the best position found by its neighborhood during the search $\vec{n_i}(t)$. The original PSO updates the velocities of the particles considering the current value for the velocity of the particles. Clerc and Kennedy [9] observed that this PSO version can present unstable operation if the parameters of the equation used to update the velocity of the particles are not properly selected. Thus, they determined a relation based on the constriction factor (χ) given in Equation (1) that avoids the explosion state. The constriction factor was designed to adjust the influence of the previous particle velocities on the optimization process. This factor also helps to switch the search mode of the swarm from exploration to exploitation during the search process. The velocity and the position of every particle are updated iteratively by applying the follow equations:

$$\chi = \frac{2}{|2 - \varphi - \sqrt{\varphi^2 - 4\varphi}|}, \; \varphi = c_1 + c_2, \tag{1}$$

$$\begin{aligned} \vec{v_i}(t+1) = \chi \cdot \Big\{ & \vec{v_i}(t) + r_1 c_1 [\vec{p_i}(t) - \vec{x_i}(t)] \\ & + r_2 c_2 [\vec{n_i}(t) - \vec{x_i}(t)] \Big\}, \end{aligned} \tag{2}$$

$$\vec{x_i}(t+1) = \vec{x_i}(t) + \vec{v_i}(t+1). \tag{3}$$

where r_1 and r_2 are random numbers generated by an uniform probability density function in the interval [0,1] at each iteration for each particle for every dimension. The factors c_1 and c_2 are the cognitive and the social acceleration constants. They are non-negative constants and weigh the contribution of the cognitive and social components.

1) Swarm Topologies: The particles only share information with the ones in their neighborhood in the swarm topology. Thus, the way the information flows through the particles is determined by the communication topology used by the swarm.

Some factors on the topology structure influence the flow of information between the particles. Kennedy and Mendes showed that when the average distance between nodes is too short, the population tends to move quickly towards the best solution found in earlier iterations [4] leading a faster convergence to the global optimum in unimodal problems. However, this fast convergence might prematurely reach a local optimum, specially in multimodal problems [3]. This is a case where communication topologies with fewer connections may yield better results because the information spreads slowly; there is a higher chance to explore different regions.

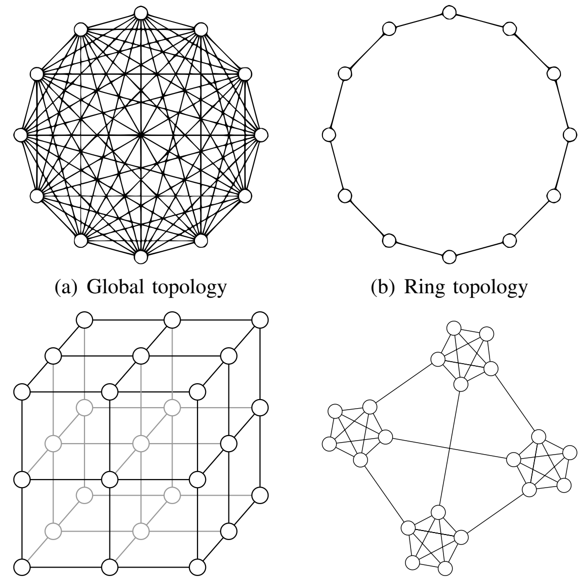

(a) Global topology (b) Ring topology (c) von Neumann topology (d) Four clusters topology

Fig. 1. The swarm topology bounds the particles communication. In the graphs for each topology, the nodes are the particles and the links represent the possibility of information exchange.

Figure 1 depicts some structures of swarm topologies. The global topology, shown in Figure 1(a), was the first communication scheme proposed for the PSO [1]. In this topology, all particles of the swarm are neighbors, that is, all particles can be the information spreader to all the other particles. Thus, the social memory of the particles is shared by the entire swarm.

Conversely, local topologies are the ones in which the particles have different subset of neighbors [3]. In this case, the social memory is not the same for the whole swarm. The topology depicted in Figure 1(b) is the most used local topology, called ring topology. The particles in this topology can only communicate with two other particles. This structure is known for helping to avoid premature attraction of the whole swarm to a single spot of the search space, because the information spreads slowly but with the caveat of a slow convergence time [3].

The dichotomous behavior of global and ring topologies suggests to consider structures to balance their strengths and weaknesses. Actually, many efforts have been made to propose approaches that present fast convergence while avoiding sub-optimal points, as depicted in Figure 1(c) and Figure 1(d), respectively, the von Neumann topology and the four clusters topology [3], [4], [10]. However, these structures are usually more suited to specific problems, mostly because they are normally based on arbitrary static structures [4].

Oliveira et al. [11] proposed a dynamic self-adaptive topology based on the preferential attachment mechanism used in the Barabási-Albert model [12]. The preferential attachment occurs because each particle tries to find the best particles to be connected. We call this topology the dynamic topology throughout this paper.

The adaption of the structure of the dynamic topology is based on the state of the swarm. In other words, when the swarm is getting stagnated, the swarm tries to modify the way the information flows aiming to optimize the search process. In order to keep track of the swarm state, each particle has a new attribute, called P_k*failures*, which keeps the number of times a particle k does *not* improve its fitness. If the particle k does not improve its position in the current iteration, P_k*failures* is incremented, otherwise P_k*failures* is set to zero.

A particle tries to find a new particle to connect to when P_k*failures* reaches a preset value: the P_k*failures* threshold. This preferential attachment is implemented by using a roulette wheel based on the rank of the particles' fitness, thus the best particles have a higher chance to be selected as connections. More details about the Dynamic topology can be found in [11].

B. The Swarm Influence Graph

The swarm topology defines which particles can communicate with one another, *i.e.* the topology only bounds the particles communication range. Thus, this structure is static and does not show the actual information flowing through the connections. The information flow changes at each iteration when a particle selects its best neighbor and retrieves information from it. Hence, at iteration t, each particle i gets information from only its best neighbor $n_i(t)$, albeit the swarm topology features many connections among particles. Therefore, the swarm topology structure is not enough to capture the information flow within the swarm.

Oliveira et al. [7] proposed the use of the swarm influence graph to understand the actual information flow. In order to represent the connections between nodes, the adjacency matrix is used with the entries (i, j) equals to 1 if the nodes i and j are connected, and 0 otherwise. Hence, the elements of the swarm influence graph I'_t at iteration t can be defined as follows:

$$I'_{t_{ij}} = \begin{cases} 1, & \text{if} \quad n_i(t) = j, \\ 0, & \text{otherwise.} \end{cases} \tag{4}$$

This definition leads to a directed graph, where the edges represent the presence of information exchange between particles with the direction of this exchange. The simplified influence graph I_t is defined by removing the edges direction. The elements of this graph at iteration t is described as follows:

$$I_{t_{ij}} = \begin{cases} 1, & \text{if} \quad n_i(t) = j \quad \text{or} \quad n_j(t) = i, \\ 0, & \text{otherwise.} \end{cases} \tag{5}$$

The influence graph I_t, as defined, consists of a set of trees and each tree represents an information flow through the swarm at iteration t. Figure 2 depicts examples of influence graphs (in bold) over three different swarm topologies. These simple examples suggest that the structure of the influence graph is very dependent of the swarm topology. For instance, one can observe that there are some sub-graphs in the ring and dynamic topologies, whereas the global topology presents a focal point in the influence graph.

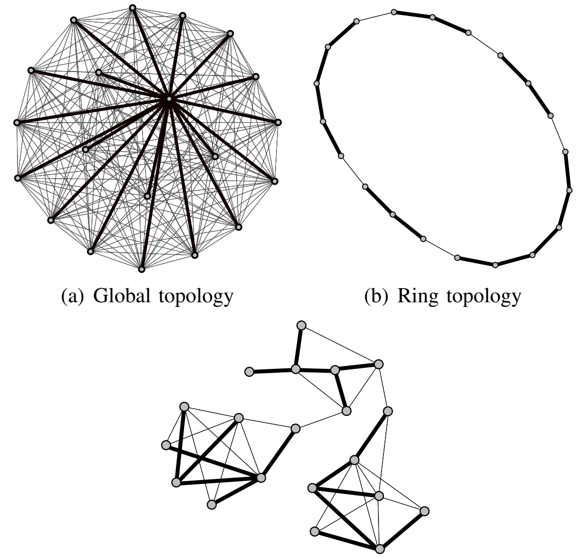

(a) Global topology (b) Ring topology

(c) Dynamic topology

Fig. 2. Examples of influence graphs over the topology for the three communication topologies. All the edges are the ones from the swarm topology, the bold edges are the actual edges of the influence graph in a certain iteration. These simple examples suggest the structure of the influence graph is very dependent of the swarm topology.

One may notice that the influence graph, as defined, captures only the instantaneous communication between particles at iteration t. Therefore, the information exchange that happened in past iterations are not present in this graph. For instance, the structure of the influence graph of the global topology is static along the iterations [7]. This particular behavior is result of the fact that only one particle spreads information at each iteration[1], which always leads to star-like structures with possibly different focal nodes at different iterations.

However, Oliveira et al. [7] showed that characteristics of the way information is transmitted within the swarm can be assessed by using the simple version of the influence graph. Although this definition enlighten some features of the information flow in the swarm depending on its topology, the presence of the social memory history in the swarm influence might explain some more intricate flow features. For example, the formation of historical information flows influencing the swarm behavior cannot be assessed with this simple definition of the influence graph.

III. The Swarm Influence Graph with History

The record of all the information exchanges between the particles during the algorithm execution until an iteration t may be evaluated by summing up the adjacency matrices from the influence graphs for all iterations before t. The matrix resulting from this sum is a weighted influence graph I_t^w. This matrix can be expressed as follows:

$$I_t^w = \sum_{i=1}^{t} I_i. \tag{6}$$

[1]Actually two particles spread information at each iteration in the global topology: the best particle $gbest$ in the swarm and the best neighbor of $gbest$. Nevertheless, the swarm influence graph still is a star-like structure.

Given that the edges of the simplified swarm influence graph I_t are undirected, I_t^w is also undirected. I_t^w is a weighted graph where its edges' weights $I_{t_{ij}}^w$ are equal to the number of the times two particles i and j exchanged information during the algorithm execution. Thus, the maximum value an edge weight can be is $2t$; this happens when two particles are always their best neighbors. The reason the weighted influence graph is created based on the undirected graph I_t and not on the directed I_t' is due to the fact that I_t is shown to have enough information to capture features from the information flow [7]. Moreover, the analysis of the structure of a undirected graph is simpler than a directed one.

The analysis of the I_t^w allows one to understand the influence of particles on each other during the whole history of the swarm. This social memory is surely related to the particles behavior until the iteration t. However, a question that may arise is the difference between the influence of an information exchange of two particles in the beginning of the process and at the iteration t. In order to allow the analysis of this dynamics, the weighted influence graph at iteration t with window t_w is defined as follows:

$$I_t^{t_w} = \sum_{i=t-t_w+1}^{t} I_i, \quad \text{with} \quad t \geq t_w > 0. \tag{7}$$

That is, $I_t^{t_w}$ is the network of particles that communicated at most t_w iterations before the iteration t. The weight of a connection between particles is equal to the number of times two particles shared information. $I_t^{t_w}$ is equal to I_t^w when $t_w = t$, and $I_t^{t_w} = I_t$ when $t_w = 1$, hence the definition with the interval window is more general, and the one used in the paper.

The size of the interval window t_w changes the analysis of $I_t^{t_w}$. The lower the value of t_w, the shorter the social memory being analyzed. A short social memory may represent only a fleeting glimpse of the information flow. Thus, the state of the flow captured using a small t_w may be only transitory. On the other hand, a large social memory may lead to analyses that takes into account remote particles interactions, which may not affect the current swarm state.

In this paper, the weighted influence graphs are analyzed using the heat map of the edges weight, the node strength (*i.e.* the sum of all edges weight connecting a node [13]) distribution and the impact of the removal of the edges on the graph components. More details on these analyses are given in Section IV-B.

IV. Simulation Setup and Results

In order to assess the proposed methodology, the PSO algorithm was run with the parameters presented in Section IV-A. The result and some preliminary analyses are given in Section IV-B.

A. PSO Setup

The PSO algorithm was run to optimize a well known multimodal benchmark function, named F_6 *function* [14]. The F_6 *function* is a shifted, single-group m-rotated and m-nonseparable Ackley's function with global optimum $x^\star = \mathbf{o}$, $F_6(x^\star) = 0$. In all experiments, the number of dimensions was set to 1000 and m equals to 50. The swarm contained 100 particles in all simulations. The simulations were made with the global, ring, von Neumann and dynamic topologies. In the case of the dynamic topology, the threshold of failures for the particles was set to P_k*failures*=50. We chose this value since it provided the best results for the entire set of benchmark functions. The particles were updated according to the Equation (2) with $c_1 = 2.05$ and $c_2 = 2.05$ as indicated in [9], which guarantees the algorithm to converge.

B. Results

Figure 3 depicts the weighted swarm influence graph with $t_w = t$ and $t = 1000$ for each topology considered. In the graph, the size of the nodes and the edges width are proportional, respectively, to the node strength and to the edges' weight. Some features for each graph may be already captured from these figures. The dense graph related to the global topology suggests a swarm behavior where all particles are exchanging information to all others. The presence of many nodes with large sizes, in the case of global and ring topologies, indicates the presence of great information spreaders in swarms with these topologies. Deeper analyses regarding these aspects are made using heat maps and the node strength distribution, given in Section IV-B1 and Section IV-B2, respectively.

In order to capture the existence of different information flows within the swarm, the weighted swarm influence graph is analyzed by removing its weak connections. Figure 4 depicts the impact of this removal regarding the von Neumann topology. This deletion of edges with weight lower than an increasing threshold shows the presence of nodes that are more tightly connected. These components (*i.e.* the sub-graphs in

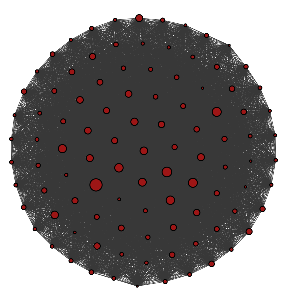

(a) Global topology

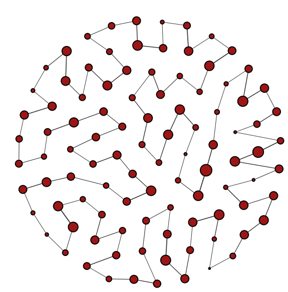

(b) Ring topology

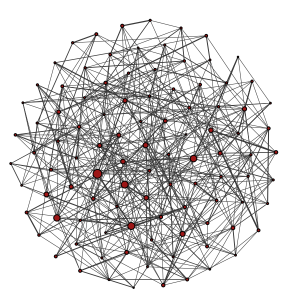

(c) Dynamic topology

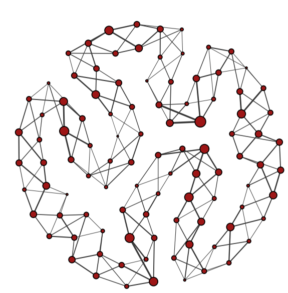

(d) von Neumann topology

Fig. 3. The weighted swarm influence graphs ($t_w = t = 1000$) are also very dependent of the used topology. The structure for the global topology (a) is denser than the other ones, and the size of the nodes (node strength) in the ring and von Neumann topologies does not change much, which hints to absence of hubs.

the case of these undirected graphs) may be seen as different flows of information in the swarm. The analysis of this aspect is given in Section IV-B3.

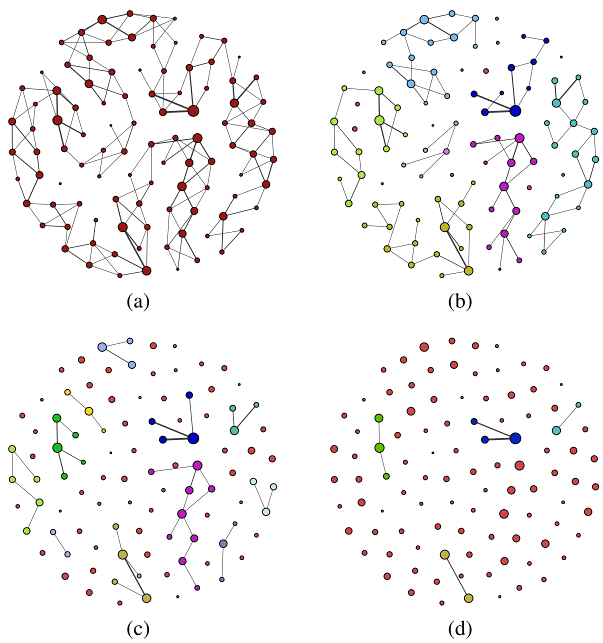

Fig. 4. The removal of low weighted edges shows the substructures within the information flow in the swarm. The weighted influence graph for the von Neumann topology in Figure 3(d) is destroyed by removing the edges with weight bellow (a) 50% of the highest edge weight, (b) 65%, (c) 75% and (d) 87.5%. The different colors are related to different components with more than one node, the size of each node is proportional to the node strength, as well as, the edges width are proportional to the edges weight.

1) Heat maps: The strength of the ties in the influence graph may be seen in the heat maps of the graph edge weights in Figure 5. Due to space limitation, only the influence graph with time window equals to 1000 and 50 are shown. The ring topology and the *von* Neumann topology show patterns due to the rules that create the swarm structure (for instance, in the ring topology, the particle i communicates only with the particles with indexes $i+1$ and $i-1$), thus these patterns are arbitrarily rule dependent. The color of each cell in the heat maps is linked to the strength of the ties between the particles. Thus, reddish cells are associated to strong ties while the blueish ones are related to weak ties.

The whole history of the information exchange in the swarm is taken into account when the window size is equal to 1000, once the snapshot is taken at the 1000$^{\text{th}}$ iteration. Some remarkable features are found on the heat maps of each influence graph for each swarm topology. In the case of the dynamic topology, although the structure changes along iterations, the initial topology has a huge influence in its social memory. This influence may be seen when one compares the patterns found in the ring topology and in the dynamic one. This comparison also allows one to visualize the presence of the new ties created during the self-adaptation process of the topology.

Although the ring and the von Neumann topologies show similar patternn, they differ in the intensity of their ties. The information exchange in the ring topology is more intense than in the von Neumann topology. This high intensity happens due to the small number of particles that one particle can communicate with in the ring topology, which leads to information exchange with only few particles.

Interestingly, none of these three aforementioned heat maps suggests the presence of particles acting as huge information spreader or a hub. On the other hand, the heat map of the global topology shows some columns with high intensity that are particles acting as actual hubs spreading information to the rest of the particles. Another characteristic of this heat map is the higher density when compared to the others. This high

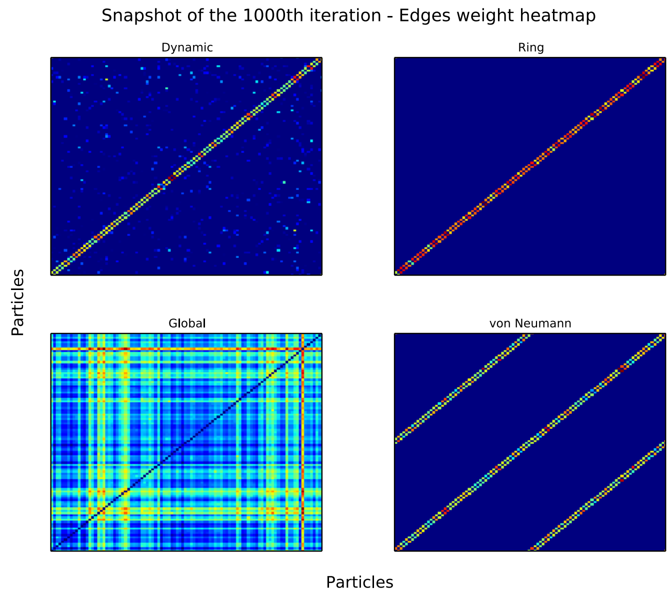

(a) Window size equals to 1000.

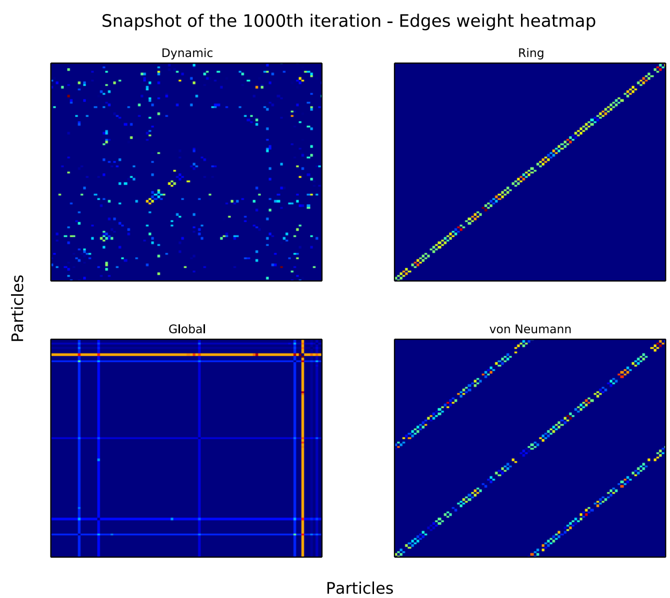

(b) Window size equals to 50.

Fig. 5. The heat map of the edges weight in the influence graph with windows size equals to (a) 1000 and (b) 50. Each column/row is a particle and the cell color is the strength of the ties between the particles. The diagonal seen in the ring topology is also seen in the dynamic topology, but this structure is lost when the window size is low.

density suggests a more dense influence graph, which means that many particles share information to many others, despite the presence of hubs.

The window size adjusted to 50 presents a slightly different picture of the swarm communication. The high density found in the global topology with window size equals to 1000 changes to a more sparse matrix. However, this heat map still shows clearly the presence of a big hub and some other small hubs as well. The comparison between these two window sizes suggests that different particles acting as a hub appears along the execution of the algorithm.

In the dynamic topology, the traces from the initial topology are not noticeable. That is, the more recent social memory does not include information exchanges through the links from the ring topology (initial topology), rather the communication is made using the new ties created during the self-adaptive process of the dynamic topology.

The heat maps of the ring and the von Neumann topologies show that the particles tend to have a preferable neighbor when the window size is small, that is, when the social memory is considered short. In the ring topology, this preference tends to create different flows of information. These flows can be seen as the contiguous lines (*i.e.* without low intensity values) in the heat map. The same feature is harder to be seen in the von Neumann topology due to the emergence of a more complex pattern, but low intensity values are still possible to be seen.

2) Nodes strength: The distribution of the strength of the nodes in the swarm influence for each swarm topology is shown in Figure 6. The plots are only for the influence graph with the window size equals to 1000. The *x-axis* limits are the same for all plots in order to have a comparison among the distributions.

The distributions for the global topology and the dynamic topology show the presence of nodes that share much information in the swarm, that is, there are some particles that are really stronger than the rest of the particles. However, these

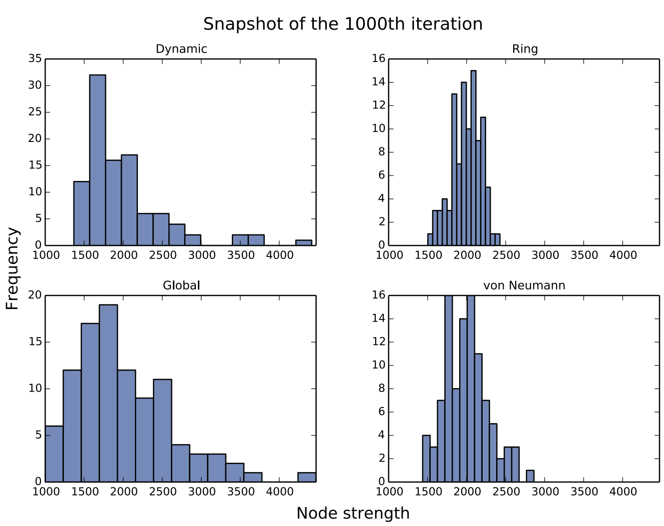

Fig. 6. The distribution of the strength of the nodes in the influence graph indicates the presence of strong nodes (hubs) in the global topology and in the dynamic topology.

information spreaders are not present in the ring topology and in the von Neumann topology. In these cases, the distribution is more concentrated in a certain region and the distribution tail is not as long as the global and dynamic topology. Still, although the distributions of the von Neumann and the Ring topologies are approximately similar in shape, the von Neumann topology presents a bigger interval strength of the nodes when compared to the ring topology. This last comparison is better seen in the complementary cumulative distribution function plot in Figure 7.

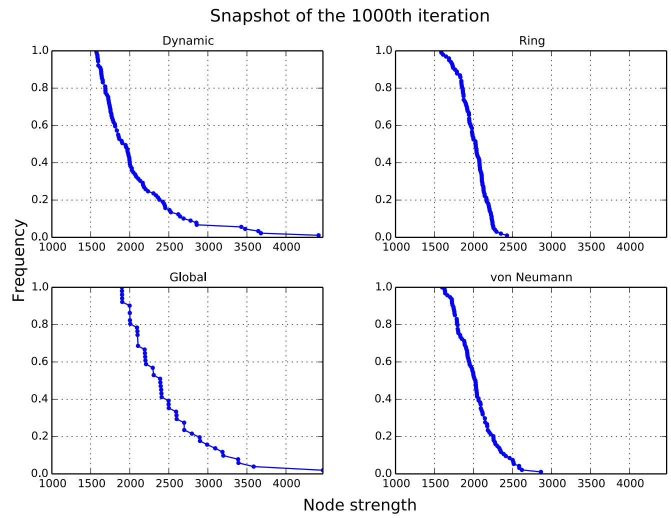

Fig. 7. The complementary cumulative distribution function of the nodes strength shows that the probability of a node being strong decays faster in the Ring topology and in the von Neumann topology than in the other topologies.

The complementary cumulative distribution function $p(X \geq x)$ describes the probability that a node will be found to have strength more than or equal to a value x. For example, although the ring and the von Neumann topologies have similar curves, the von Neumann topology has a slightly longer tail, which means that a hub is slightly easier to happen in this topology than in the Ring topology. Yet, in both topologies, the probability of a node being strong decays faster than in the dynamic and the global topologies. This slow decay in the probability is a consequence of the presence of hubs in the information flow, a feature which is related to less diversity.

Figure 8 presents a comparison of the nodes strength distributions of the influence graph with the time window size equals to 10, 100, 500 and 1000 for each swarm topology considered. This comparison shows that the presence of hubs in the global topology is independent of the social memory size, that is, this topology allows the emergence of influential particles in a short time. Conversely, the curves for the dynamic topology only show hubs when the window is large. These features make both topologies prone to have particles as huge information spreaders. However, the dynamic topology takes longer to elect this particle than in the global topology, a behavior that may help the swarm to not stagnate in sub-optimal points.

3) The impact of edges removal: The decrease of the largest component size when edges are removed from the swarm influence graph for each swarm topology is shown in Figure 9(a). The impact of this removal on the number of the

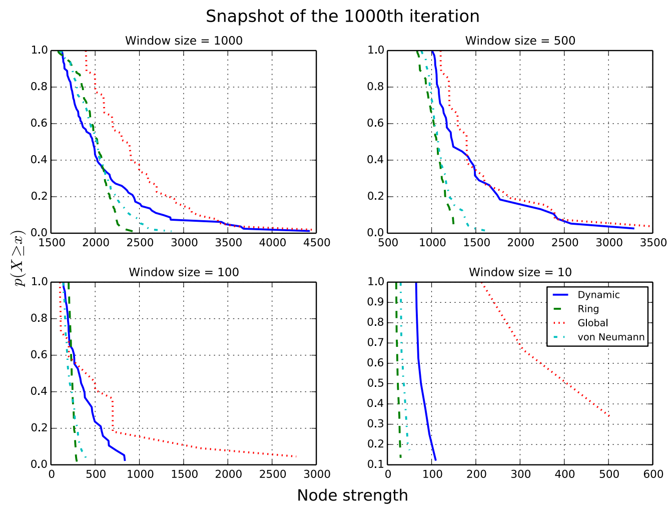

Fig. 8. The complementary cumulative distribution function of the nodes strength in the swarm influence graph with different window sizes. The curve colors/shapes are related to the swarm topology. The tail of the global topology curve is longer in all scenarios, indicating the presence of hubs independent of temporal constraint.

components in the graph is shown in Figure 9(b). In order to make the plots understandable and due to space limitation, only the window sizes equal to 10, 50, 100, 500 and 1000 are presented, which are represented by different colors/markers. The normalized weight is the weight value divided by $2t_w$, *i.e.* the highest possible weight in the graph. The giant component size is equal to the number of nodes in the largest component divided by the total number of nodes. In the plots, the markers are the actual values of the normalized weights, that is, the curves just connect the markers and the lines only help to understand the tendency.

The impact of the edges removal on the size of the greatest flow of information in the case of the global topology does have similar behavior with different window sizes. The giant component is completely destroyed in few steps. This behavior in conjunction with the rapidly increasing of the number of components during this removal suggests the absence of different flows of information and the presence of the only one flow, the greatest one. This characteristic indicates that the global topology does not have high diversity, thus the swarm is guided by the same information, which leads to the particles moving towards the same place. This behavior of the swarm is related to the exploitation search mode.

On the other hand, the curves in the von Neumann topology and the ring topology cases for the giant component size have distinct behaviors with different window sizes. The greatest information flow in both topologies does not contain all the particles when the window size is equal to 10, 50 and 100. This behavior is in agreement with the heat maps for these topologies with a short social memory, that is, when the history is from a short period of the past iterations, the swarm has different flows of information. The von Neumann topology does have, however, longer greatest information flow than the ring topology for window size equals to 50 and 100, which suggests that the von Neumann topology tends to have less diversity in flows of information than the ring topology.

In the case of window size equals to 500 and 1000, the curves regarding the giant component size for the ring topology and von Neumann topology shows that the greatest information flow includes all the particles. However, the edges removal leads to a faster destruction in the case of the von Neumann topology than in the ring topology case, which points again to a less diversity in the von Neumann topology. This fast destruction in both cases must be analyzed with the growth of number of components. For instance, in relation to the global topology, the number of components increases quickly when the edges are removed. However, in the case of the other topologies, the quantity of components increases slowly. Therefore, the giant component in these topologies is destroyed in many components and not in many nodes, which indicates that the swarms with these topologies contain many different flows of information (*i.e.* different sub-swarm searching independently within the search space).

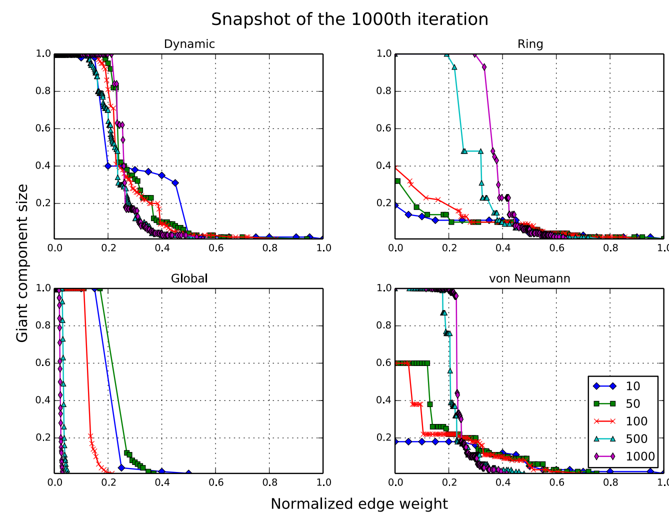

(a) The size of the giant component.

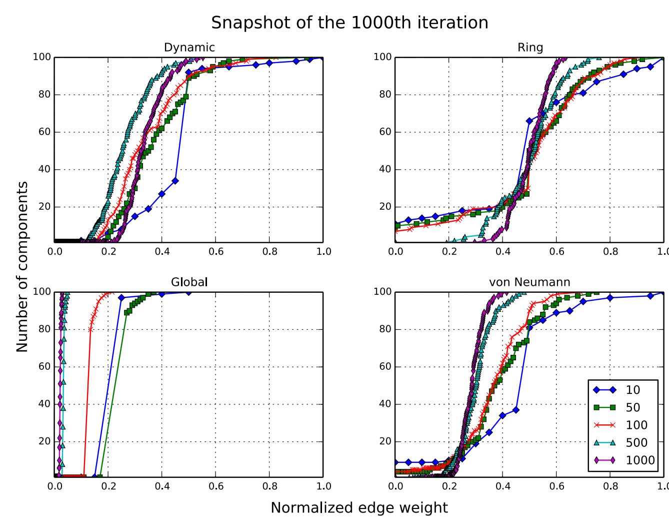

(b) The number of components.

Fig. 9. The impact of the edges removal on the size of the giant component (a) and on the growth of the number of components (b) depends on the network structure. The different curves (the different colors/markers in the plot) are related to the time window size of the influence graph.

The dynamic and the von Neumann topologies have similar behaviors when the window is set to 500 and 1000. However, as mentioned before, the greatest information flow in the swarm with the von Neumann topology does not contain all the particles when the window is equal to 10, 50 and 100. On the other hand, the Dynamic topology, allows the swarm to have a long information flow with all the particles with these time window sizes. This phenomenon suggests that the dynamic topology is not as diverse as the von Neumann topology when the social memory is short.

V. Conclusion and Future Works

We defined a network-based approach to represent the particles interactions, namely the weighted swarm influence graph $I_t^{t_w}$, and we showed that the search behavior in PSO can be assessed by analyzing the properties of this graph. The benefit of this approach is that we do not use any particles properties (*e.g* the position of a particle, the velocity of a particle, etc) for the analysis, and we can have richer assessments in terms of information about the flows within the swarm than the usual approaches.

The analysis we performed was concerned with strongly connected components and the distribution of the nodes strength in influence graphs. We associated a component in the graph to an information flow in the network, further we related the number of these components with the swarm diversity. Moreover, we used the nodes strength as an indication of the presence of influential particles in the swarm, that is also related to the diversity in the information flow.

The hub analysis of swarm influence graph demonstrated that in a swarm with the global topology, there is a strong presence of particles as large information spreaders, a feature related to less diversity. These strong hubs also appeared in the dynamic topology, but not in the von Neumann and the ring topologies. In this case, the characteristic distinguishing the global and the dynamic topologies is that the former allows the emergence of influential particles in a short time, while the latter takes longer to elect a particle as a hub. This delayed behavior may help the swarm to not stagnate in local optima.

The analysis on the influence graph edge weights showed that there exists only one information flow in a swarm with the global topology, a behavior associated to the exploitation search mode. Conversely, in the von Neumann, ring and dynamic topologies, the swarms contain different flows of information, which drives the swarm to explore distinct places in the search space, a feature related to the exploration search mode. The difference between these two topologies is that the ring topology has higher diversity in terms of information flow than the von Neumann topology, and the latter tends to have a more diverse swarm than the dynamic topology.

For future works, we envisage a network-based framework to assess the swarm behavior in different swarm intelligence techniques. This framework might give us comprehension on the intricate interactions within the swarm, that could lead us, for example, to more general descriptions and classifications of swarm techniques. However, our definition is still not generic enough, an example of this fact is that, even if $c_2 = 0$ in Equation (2) (*i.e.* particles do not communicate) – a scenario that could happen when c_1 and c_2 are adaptive – the influence graph does have ties between the particles. Therefore, our next steps are towards an influence graph definition that allows a more generic and less descriptive analysis.

Acknowledgment

Marcos Oliveira would like to thank the Science Without Borders program (CAPES, Brazil) for financial support under grant 1032/13-5.

References

[1] J. Kennedy and R. Eberhart, "Particle swarm optimization," vol. 4, 1995, pp. 1942–1948 vol.4. [Online]. Available: http://dx.doi.org/10.1109/ICNN.1995.488968

[2] R. Mendes, J. Kennedy, and J. Neves, "The fully informed particle swarm: simpler, maybe better," *Evolutionary Computation, IEEE Transactions on*, vol. 8, no. 3, pp. 204 – 210, june 2004.

[3] D. Bratton and J. Kennedy, "Defining a standard for particle swarm optimization," *Swarm Intelligence Symposium, 2007. SIS 2007. IEEE*, pp. 120 –127, april 2007.

[4] J. Kennedy and R. Mendes, "Population structure and particle swarm performance," in *Evolutionary Computation, 2002. CEC '02. Proceedings of the 2002 Congress on*, vol. 2, 2002, pp. 1671 –1676.

[5] J. Kennedy and R. C. Eberhart, *Swarm Intelligence*. San Francisco, CA, USA: Morgan Kaufmann Publishers Inc., 2001.

[6] M. Clerc and J. Kennedy, "The particle swarm - explosion, stability, and convergence in a multidimensional complex space," *Evolutionary Computation, IEEE Transactions on*, vol. 6, no. 1, pp. 58–73, 2002. [Online]. Available: http://dx.doi.org/10.1109/4235.985692

[7] M. Oliveira, C. Bastos-Filho, and R. Menezes, "Assessing particle swarm optimizers using network science metrics," in *Complex Networks IV*, ser. Studies in Computational Intelligence, G. Ghoshal, J. Poncela-Casasnovas, and R. Tolksdorf, Eds. Springer Berlin Heidelberg, 2013, vol. 476, pp. 173–184. [Online]. Available: http://dx.doi.org/10.1007/978-3-642-36844-8_17

[8] O. Olorunda and A. P. Engelbrecht, "Measuring exploration/exploitation in particle swarms using swarm diversity," in *2008 IEEE Congress on Evolutionary Computation (IEEE World Congress on Computational Intelligence)*. IEEE, June 2008, pp. 1128–1134.

[9] M. Clerc and J. Kennedy, "The particle swarm - explosion, stability, and convergence in a multidimensional complex space," *Evolutionary Computation, IEEE Transactions on*, vol. 6, no. 1, pp. 58 –73, feb 2002.

[10] R. Mendes, J. Kennedy, and J. Neves, "Watch thy neighbor or how the swarm can learn from its environment," in *Swarm Intelligence Symposium, 2003. SIS '03. Proceedings of the 2003 IEEE*, april 2003, pp. 88 – 94.

[11] M. Oliveira, C. J. A. Bastos-Filho, and R. Menezes, "Using network science to define a dynamic communication topology for particle swarm optimizers," in *Complex Networks*, ser. Studies in Computational Intelligence, R. Menezes, A. Evsukoff, and M. C. González, Eds. Springer Berlin Heidelberg, 2013, vol. 424, pp. 39–47.

[12] R. Albert and A.-L. Barabasi, "Statistical mechanics of complex networks," *Reviews of Modern Physics*, vol. 74, p. 47, 2002. [Online]. Available: doi:10.1103/RevModPhys.74.47

[13] A. Barrat, M. Barthelemy, R. Pastor-Satorras, and A. Vespignani, "The architecture of complex weighted networks," *Proceedings of the National Academy of Sciences of the United States of America*, vol. 101, no. 11, pp. 3747–3752, 2004.

[14] K. Tang, X. Li, P. N. Suganthan, Z. Yang, and T. Weise, "Benchmark Functions for the CEC'2010 Special Session and Competition on Large-Scale Global Optimization," University of Science and Technology of China (USTC), School of Computer Science and Technology, Nature Inspired Computation and Applications Laboratory (NICAL): China, Tech. Rep.